

## Luminescence and Vibrational Spectra of $Ba_5Li_2W_3O_{15}$

G. BLASSE

*Solid State Chemistry Department, Physical Laboratory, State University, Utrecht, The Netherlands*

Received October 8, 1974

The infrared and Raman spectra of  $Ba_5Li_2W_3O_{15}$  are reported down to  $200\text{ cm}^{-1}$ . From the internal stretching modes of the tungstate octahedra the crystallographic order between lithium and tungsten in the face-sharing octahedra can be derived. The green tungstate luminescence shows a low quenching temperature that is described with the Dexter-Klick-Russell model. The  $U^{6+}$  ion shows a yellow emission in  $Ba_5Li_2W_3O_{15}$ . There is ample evidence for two different  $U^{6+}$  centers with different decay times (10 and  $80\ \mu\text{sec}$ ) and different emission and excitation spectra. One of these is located in a single layer of tungstate octahedra, the other in a double layer of octahedra.

### 1. Introduction

Recently interest has grown in perovskite-related compounds of the type  $Ba(Li, M)O_3$  where M is a highly charged cation like  $Nb^{5+}$ ,  $W^{6+}$ , or  $Sb^{5+}$  (1-4). If M has a noble-gas configuration, the stacking sequence of  $BaO_3$  layers is not cubic and pairs of face-sharing octahedra occur. The compound  $Ba_5Li_2W_3O_{15}$ , for example, has a 10-layer crystal structure (1, 2). If M has a  $d^{10}$  configuration, the  $BaO_3$  stacking sequence is cubic.

In the course of our studies on the luminescence and vibrational spectra of tungstates and related compounds it seemed interesting to study the optical properties of  $Ba_5Li_2W_3O_{15}$ . In this paper we report vibrational spectra that prove an additional detail of the crystal structure and luminescence spectra. Further we studied the luminescence of  $U^{6+}$  in this compound because this activator shows efficient luminescence in tungstate perovskites (5).

### 2. Experimental

Samples were prepared as described in the literature (1, 2). They were checked by X ray analysis. The performance of the vibrational

and luminescence spectra has been described previously (6).

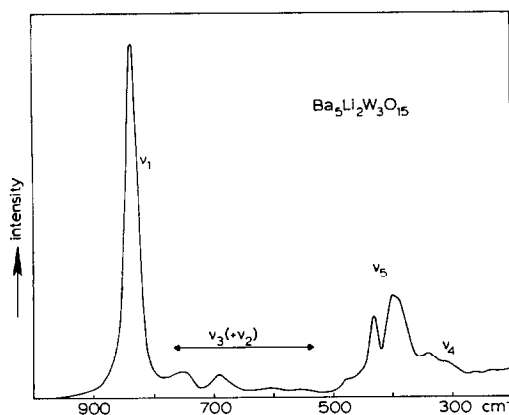
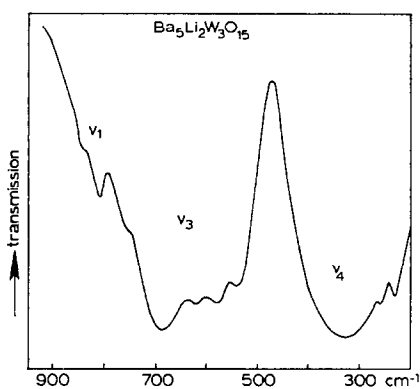
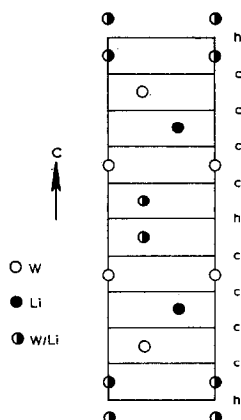
### 3. Results and Discussion

#### a. Vibrational Spectra

In Figs. 1 and 2 the Raman and infrared spectra of  $Ba_5Li_2W_3O_{15}$  are presented. In view of our earlier work on ordered perovskites of the type  $A_2BWO_6$  (7, 8) it is easy to indicate to which of the internal vibrational modes of the  $WO_6$  octahedron the observed bands are related. This is done in Figs. 1 and 2.

In view of the complicated crystal structure, a complete assignment of all vibrational bands is neither an easy nor a useful task. We feel, however, that the present spectra reveal a structural detail.

The crystal structure of  $Ba_5Li_2W_3O_{15}$  consists of a 10-layer stacking of  $BaO_3$  layers with sequence *hcccccccc* (1, 2).  $Li^+$  and  $W^{6+}$  ions occupy the centers of oxygen octahedra in such a way that strings of three corner-sharing octahedra are linked by corners to face-sharing pairs of octahedra (see Fig. 3). In the strings, the center octahedron is occupied by lithium, the other two by tungsten. The occupation of the pairs with equal amounts

FIG. 1. Raman spectrum of  $\text{Ba}_5\text{Li}_2\text{W}_3\text{O}_{15}$ .FIG. 2. Infrared spectrum of  $\text{Ba}_5\text{Li}_2\text{W}_3\text{O}_{15}$ .FIG. 3. Hexagonal (110) view of the octahedral cations in  $\text{Ba}_5\text{Li}_2\text{W}_3\text{O}_{15}$ . The  $\text{BaO}_3$  layers have been omitted. They are indicated by  $h$  and  $c$  (hexagonal and cubic close packed layer, respectively).

of lithium and tungsten cannot be proved from Bragg reflection data (2). We will show now that our spectra give strong evidence that the pairs contain one lithium and one tungsten ion in such a way that all the pairs in a layer perpendicular to the  $c$ -axis have equal occupation.

If the pair distribution were random (even with one lithium and one tungsten in one pair) the number of  $\text{WO}_6$  octahedra with different surroundings would be large. As a consequence broad and unstructured spectra would be expected. This is definitely not the case. The order proposed above can explain the spectra observed experimentally in a qualitative way.

If all pairs in a layer perpendicular to the hexagonal  $c$ -axis are occupied equally by one  $\text{Li}^+$  and one  $\text{W}^{6+}$  ion, two types of  $\text{WO}_6$  octahedra can be distinguished:

(a) A layer of  $\text{WO}_6$  octahedra sharing corners with six  $\text{LiO}_6$  octahedra. The trigonal field at these  $\text{WO}_6$  octahedra must be weak and their vibrational spectra will resemble those of the ordered perovskites  $\text{A}_2\text{BWO}_6$  (7, 8).

(b) Double layers of  $\text{WO}_6$  octahedra (see Fig. 3). There is a strong trigonal field at each of these octahedra. It is not easy to predict their spectrum but the trigonal field should be discernible in the spectra as observed before in a similar situation [ $\text{Sr}_3\text{MgNb}_2\text{O}_9$ , ref. (9)].

We now turn to the spectra. In Table I we have given a prediction of intensity and position of the bands expected for the single and double layers of  $\text{WO}_6$  octahedra in comparison with experimental results. For a regular  $\text{WO}_6$  group the  $\nu_1$  mode ( $A_{1g}$ ) is infrared-forbidden and Raman-allowed, whereas the  $\nu_3$  mode ( $T_{1u}$ ) is infrared-allowed and Raman-forbidden. For the single layer of  $\text{WO}_6$  octahedra with weak trigonal field and coordination comparable to that of the 1:1 ordered perovskites  $\text{A}_2\text{BWO}_6$  we expect a strong  $\nu_1$  in the Raman spectrum and a strong  $\nu_3$  in the infrared spectrum at the same position as, for example, in  $\text{Ba}_2\text{MgWO}_6$ . Due to the trigonal field ( $C_{3v}$ ) the exclusion rule may be slightly lifted. With these predictions a number of assignments can be made as indicated in Table I. For the double

TABLE I  
ASSIGNMENT OF  $\text{WO}_6$  STRETCHING VIBRATIONS IN  $\text{Ba}_5\text{Li}_2\text{W}_3\text{O}_{15}$ <sup>a</sup>

Single $\text{WO}_6$ layers (Li-W-Li, weak trigonal field)		Double $\text{WO}_6$ layers (Li-W-W, strong trigonal field)	
Prediction <sup>b</sup>	Observation	Prediction	Observation
Infrared			
$\nu_1$ (very weak) 820	840 (vw)	$\nu_1$ (weak)	810 (w)
$\nu_3$ (strong) 620	625 (s)	$\nu_3$ (strong, several bands)	750 (m), 685 (s), 575 (s), 540 (s)
Raman			
$\nu_1$ (strong) 820	835 (s)	$\nu_1$ (strong)	835 (s)
$\nu_3$ (very weak) 620	610 (vw)	$\nu_3$ (weak, several bands)	750 (w), 690 (w), 560 (vw)

<sup>a</sup> All values are in  $\text{cm}^{-1}$ .

<sup>b</sup> Predicted frequencies from (7) and (8).

layers, the situation is more complicated, the situation is more complicated, but in comparison with the single layers there should be a considerable splitting of  $\nu_3$  (more than  $100 \text{ cm}^{-1}$ , as in  $\text{Sr}_3\text{MgNb}_2\text{O}_6$ ) and a stronger deviation from the exclusion rule. The assignment given in Table I is not in contradiction with these predictions.

#### b. Luminescence of Undoped $\text{Ba}_5\text{Li}_2\text{W}_3\text{O}_{15}$

Undoped samples of  $\text{Ba}_5\text{Li}_2\text{W}_3\text{O}_{15}$  show a greenish photoluminescence of low to medium intensity at temperatures below about  $75^\circ\text{K}$ . Fig. 4 shows the excitation and emission spectra at  $5^\circ\text{K}$ . The excitation band peaks

at 310 nm for several emission wavelengths. The emission band peaks at 490 nm under excitation into the maximum of the excitation band. Under excitation with shorter wavelengths the emission shifts to longer wavelengths (see Fig. 4). The optical absorption edge at room temperature is situated at about 320 nm according to the diffuse reflection spectrum of the compound.

Previously it has been argued (10) that the position of this edge determines the luminescence behavior of the octahedral tungstate group. For 320 nm, that model predicts low-intensity photoluminescence with a low quenching temperature, as observed ex-

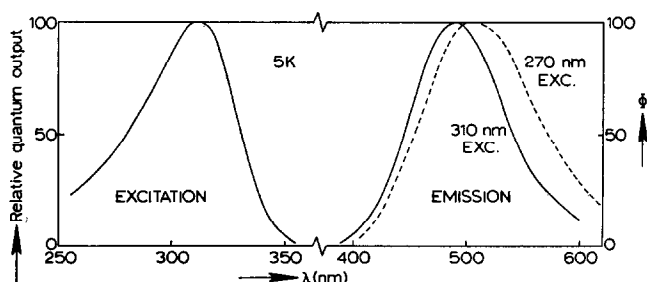


FIG. 4. Luminescence spectra at  $5^\circ\text{K}$  of  $\text{Ba}_5\text{Li}_2\text{W}_3\text{O}_{15}$ . Left-hand side: Relative excitation spectrum of the 500 nm emission. Right-hand side: Spectral energy distribution of the emission under 310 nm and 270 nm excitation (drawn and broken line, respectively).  $\Phi$  gives the radiant power per constant wavelength interval in arbitrary units.

perimentally. The Dexter–Klick–Russell configuration coordinate model is applicable (11).

The excitation and emission bands of the luminescence show a pronounced Stokes shift of about  $12\,000\text{ cm}^{-1}$ . In view of the lack of spectral overlap the probability for energy transfer between the octahedral  $\text{WO}_6$  groups cannot be very large (12).

The emission of  $\text{Ba}_5\text{Li}_2\text{W}_3\text{O}_{15}$  must be of a complicated nature, since it depends on the excitation wavelength (Fig. 4). This is not unexpected in view of the number of crystallographically different tungstate groups. An obvious possibility is that there are two emission bands, one due to  $\text{WO}_6$  octahedra in the single layer, the other to octahedra in the double layer. A slight amount of lithium–tungsten disorder, however, may also be responsible for a double emission, in the same way as magnesium–tungsten disorder is responsible for the double emission of  $\text{Ba}_2\text{MgWO}_6$  (13). We prefer the first possibility because shorter wavelength excitation produces longer wavelength emission in contradistinction with the results of (13) and because the energy transfer probability is low. The longer wavelength emission must then be due to the  $\text{WO}_6$  groups in the double layer, since corner-sharing  $\text{WO}_6$  octahedra show emission at wavelengths longer than 500 nm (13). The shorter wavelength emission can be ascribed to the single layer octahedra. Note that the electrostatic bond strength (14) of the oxygen ions of these octahedra amounts to 11/6. In the ordered perovskites  $\text{A}_2\text{BWO}_6$  this bond strength is 2, as required by Pauling's electrostatic valence rule. We have shown earlier (15) that a low value of the electrostatic bond strength implies excitation and emission bands at relatively low energy, and consequently, low quenching temperatures of the luminescence. The ordered perovskites show emission in the blue spectral region with quenching temperatures of about  $200^\circ\text{K}$  (8, 16), so that the present values are in qualitative agreement with the theory presented before (15).

Since the  $\text{U}^{6+}$  ion proved to be an efficient activator of tungstate perovskites (5), we also investigated the behavior of  $\text{U}^{6+}$  in  $\text{Ba}_5\text{Li}_2\text{W}_3\text{O}_{15}$ .

### c. Luminescence of the $\text{U}^{6+}$ Ion in $\text{Ba}_5\text{Li}_2\text{W}_3\text{O}_{15}$

Uranium-activated  $\text{Ba}_5\text{Li}_2\text{W}_3\text{O}_{15}$  shows at room temperature and below a yellow emission of medium intensity under excitation with short and, especially, long-wavelength uv radiation.

The presence of the  $\text{U}^{6+}$  ion in  $\text{Ba}_5\text{Li}_2\text{W}_3\text{O}_{15}$  results in a characteristic broad  $\text{U}^{6+}$  excitation band peaking at about 375 nm. It extends into the visible up to about 450 nm. This band has a higher intensity than the tungsten excitation band at 310 nm so that the total probability of transfer from tungstate to uranate center cannot be very high.

At low temperatures, the  $\text{U}^{6+}$  emission shows a certain fine structure, as shown in Fig. 5, for excitation into the uranium excitation band. Excitation into the tungstate excitation band at low temperatures results in tungstate and uranate emission (Fig. 6) which indicates that energy transfer from tungstate to uranate occurs. Due to the larger slit widths applied the fine structure is no longer observable. At room temperature the structure has disappeared completely.

Note that the uranate emission maximum depends on the excitation wavelength. This is shown in Fig. 6 at  $5^\circ\text{K}$ , but the same phenomenon is observed at room temperature.

Finally we found that the decay of the uranate emission can be described with two

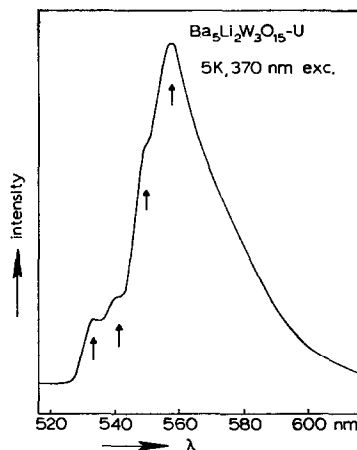


FIG. 5. Emission spectrum of  $\text{Ba}_5\text{Li}_2\text{W}_3\text{O}_{15}\text{-U}$  (uncorrected recorder curve) at  $5^\circ\text{K}$  under 370 nm excitation. Arrows indicate vibrational fine structure.

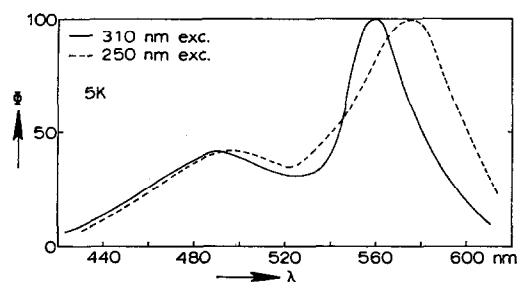


FIG. 6. Spectral energy distribution of the emission of  $\text{Ba}_5\text{Li}_2\text{W}_{2.97}\text{U}_{0.03}\text{O}_{15}$  at  $5^\circ\text{K}$ . Drawn curve: 310 nm excitation (in the optical band edge of the host lattice); broken curve: 250 nm excitation. The latter spectrum was recorded with broader slits.

exponentials with  $\tau_1 = 10 \mu\text{sec}$  and  $\tau_2 = 80 \mu\text{sec}$ . This was observed at 77 and  $300^\circ\text{K}$  and for uranate as well as tungstate excitation. In the case of tungstate excitation (280 nm) the shorter component was more intense than for uranate excitation (360 nm).

We now turn to an examination of these results. As before (5) the yellow emission is ascribed to a substitutional  $\text{UO}_6$  octahedron.

From our results above we expect that there will be two different  $\text{U}^{6+}$  centers, i.e., one in the single layers and at least one other in the double layers. This is substantiated by our experiments. First, the emission maximum varies with the excitation wavelength. Second, the decay measurements reveal two different decay times. In ordered perovskites  $\text{A}_2\text{BWO}_6$  the  $\text{U}^{6+}$  luminescence decays always by a single exponential (5, 17). Thirdly the emission spectra at  $5^\circ\text{K}$  (Fig. 5) show the presence of two zero-phonon lines at 532 and 541 nm. The fine structure in ordered perovskites (5) and compounds  $\text{M}_2\text{WO}_5$  (18) shows only one zero-phonon line. In the emission spectrum (Fig. 5) it is further possible to discern two phonon-assisted lines at 549 and 557.5 nm, respectively. The energy difference with the respective zero-phonon lines is about  $600 \text{ cm}^{-1}$ . This value agrees with the octahedral  $\nu_3$  mode of the uranate group (8). Assuming a statistical distribution of uranium among the tungsten sites the 541 nm peak (with the 557.5 nm peak) as assigned to  $\text{U}^{6+}$  in the double layers due to its higher intensity compared with the 532 nm peak (with the

549 nm peak). This assignment should be handled with care.

Finally, we consider the energy transfer between the tungstate and uranate octahedron. It was argued above that transfer between tungstate groups mutually cannot give an important contribution to the total probability for tungstate-uranate transfer.

In a sample of  $\text{Ba}_5\text{Li}_2\text{W}_3\text{O}_{15}$  in which 1% of the tungsten had been replaced by uranium it was found at  $5^\circ\text{K}$  that excitation into the tungstate groups (310 nm) resulted in emission of a roughly equal amount of tungstate and uranate quanta. It is an easy task to derive from this fact that the critical distance for energy transfer (19) from tungstate to uranate must be of the order of 15 Å, a large value for an inorganic system.

The dependence of the emission maximum of the uranate luminescence on the excitation wavelength can be explained by assuming preferential transfer from the tungstate double layer groups to the uranate group with the longer wavelength emission. This may be due to the fact that a double-layer  $\text{WO}_6$  group has, within 5–6 Å, many more double-layer  $\text{WO}_6$  neighbors than single-layer  $\text{WO}_6$  neighbors, whereas for the single-layer  $\text{WO}_6$  group their number is about equal. In view of the many uncertainties in the present system further analysis seems impossible.

Since the intensity of the 10- $\mu\text{sec}$  emission component increases on excitation in the tungstate group we conclude that the longer wavelength emission has a shorter decay time.

### Acknowledgments

The author is indebted to Mr. G. P. M. van den Heuvel for the preparation and measurements of the samples, to Dr. J. H. van der Maas for the performance of the Raman spectrum, and to Dr. J. T. W. de Hair for the decay measurements.

### References

1. T. NEGAS, R. S. ROTH, H. S. PARKER, AND W. S. BROWER, *J. Solid State Chem.* **8**, 1 (1973).
2. A. J. JACOBSON, B. M. COLLINS, AND B. E. F. FENDER, *Acta Cryst.* **B30**, 816 (1974).
3. B. M. COLLINS, A. J. JACOBSON, AND B. E. F. FENDER, *J. Solid State Chem.* **10**, 29 (1974).
4. A. J. JACOBSON, B. M. COLLINS, AND B. E. F. FENDER, *Acta Cryst.* **B30**, 1705 (1974).

5. J. T. W. DE HAIR AND G. BLASSE, *J. Luminescence* **8**, 97 (1973).
6. G. BLASSE AND G. P. M. VAN DEN HEUVEL, *Phys. Stat. Sol.* **a19**, 111 (1973).
7. A. F. CORSMIT, H. E. HOEFDRAAD, AND G. BLASSE, *J. Inorg. Nucl. Chem.* **34**, 3401 (1972).
8. G. BLASSE AND A. F. CORSMIT, *J. Solid State Chem.* **6**, 513 (1973).
9. G. BLASSE AND A. F. CORSMIT, *J. Solid State Chem.* **10**, 39 (1974).
10. G. BLASSE AND A. BRIL, *J. Solid State Chem.* **2**, 291 (1970).
11. D. L. DEXTER, C. C. KLINK, AND G. A. RUSSELL, *Phys. Rev.* **100**, 603 (1955).
12. G. BLASSE, *Philips Res. Repts.* **23**, 344 (1968).
13. J. H. G. BODE AND A. B. VAN OOSTERHOUT, *J. Luminescence*, in press.
14. L. PAULING, "The Nature of the Chemical Bond", Chap. 48, Oxford University Press, London (1952).
15. G. BLASSE AND A. BRIL, *Z. Physik. Chem. (Frankfurt)* **57**, 187 (1968).
16. A. B. VAN OOSTERHOUT, private communication.
17. J. T. W. DE HAIR AND J. F. DE ROOY, unpublished results.
18. G. BLASSE AND G. P. M. VAN DEN HEUVEL, *J. Luminescence* **8**, 406 (1974).
19. D. L. DEXTER, *J. Chem. Phys.* **21**, 836 (1953).